A BOUNDARY ELEMENT METHOD FOR OSCILLATING STOKES FLOW AT LOW FREQUENCIES AROUND A RIGID BODY

Jorge D'Elía, Laura Battaglia, Sofía Sarraf and Alberto Cardona

*Centro Internacional de Métodos Computacionales en Ingeniería (CIMEC), Instituto de Desarrollo Tecnológico para la Industria Química (INTEC), Universidad Nacional del Litoral - CONICET ,
Güemes 3450, 3000-Santa Fe, Argentina, e-mail: jdelia@intec.unl.edu.ar,
lbattaglia@santafe-conicet.gob.ar, sssarraf@gmail.com, acardona@intec.unl.edu.ar , web page:*
http://www.cimec.org.ar

Keywords: boundary-integral methods; potential theory; Fredholm integral equations; boundary element methods; Galerkin and collocation methods; low-Reynolds-number (creeping) flows.

Abstract. The unsteady creeping flow around a rigid three dimensional body at rest in an incompressible and viscous fluid of Newtonian type is considered. The flow problem is modeled using an indirect boundary integral equation (IBIE), and is numerically solved by using collocation and Galerkin weighting procedures. An IBIE was presented in a previous work for the steady creeping flow case (D'Elía *et al.*, *Mecánica Computacional*, vol. XXVIII:1453-1462, 2009), whereas in the present work the attention is focused to the oscillatory creeping flow with an harmonic time dependence. The formulation is specialized to low frequencies and boundary meshes with flat simplex triangles. The double surface integrals in the Galerkin approach that account the pairwise interaction among all boundary elements are computed on using a variation of the scheme proposed by Taylor (D. J. Taylor, IEEE Trans. on Antennas and Propagation, 51(7): 1630-1637, 2003). Numerical examples include the unsteady creeping flow with an harmonic time dependence around the sphere of unit radius and around the cube of unit edge length, both at rest, covering issues on the convergence under mesh refinement and, in the first test case, a comparison against the analytical values as a function of the imposed vibrating frequency.

1 INTRODUCTION

As it is known, the Stokes equation for a creeping flow provides a description of the fluid dynamics of a viscous fluid as long as the flow regime is laminar and attached, and the viscous forces dominate over the inertial ones. The last condition is typically satisfied when the bounding surfaces of the flow domain are relatively large compared to the bounded volume, as in microhydrodynamics, such as colloidal flows and flows around micro-electro-mechanical systems (MEMS), e.g. see Wang (2002); Méndez et al. (2008); Berli and Cardona (2009). Some devices in MEMS have intricate three dimensional (3D) bounded contours with a bounded volume of fluid.

In this work, an indirect boundary integral equation (IBIE) proposed in a previous work (D'Elía et al., 2009b) is employed for simulating the unsteady creeping flow around a rigid three dimensional isolated body at rest where the fluid performs a time-harmonic vibration at low frequencies ω and small oscillation amplitudes. The method consist of solving the unsteady creeping flow around an isolated body by applying a boundary element method (BEM) performed with collocation and Galerkin weighting procedures. The last procedure is also known as a Galerkin boundary element method (GBEM, Bonnet et al., 1998; Sutradhar et al., 2008).

2 MATHEMATICAL FORMULATION

2.1 Time-dependent Stokes equations system

The fluid velocity $v_i = v_i(\mathbf{x}, t)$ and pressure $p = p(\mathbf{x}, t)$ fields of an unsteady and creeping flow of a viscous and incompressible fluid of Newtonian type satisfy the time-dependent Stokes equations system (Kim and Karrila, 1991)

$$\rho\frac{\partial v_i}{\partial t} = \frac{\partial p}{\partial x_i} + \mu\frac{\partial^2 v_i}{\partial x_j \partial x_j} \,,$$
$$\frac{\partial v_i}{\partial x_i} = 0 \,, \tag{1}$$

for time $t \in [0, T]$, with $i = 1, 2, 3$, for all field points $\mathbf{x} = (x_1, x_2, x_3)$ in the exterior flow domain Ω^e to a closed surface A of arbitrary shape, see Fig. 1, where ρ is the fluid density and μ is the dynamic fluid viscosity. The boundary conditions include the non-slip boundary condition on the surface A given by

$$v_i(\mathbf{x}, t) + u_i(\mathbf{x}, t) = 0 \quad \text{for all } \mathbf{x} \in A \text{ and for all } t, \tag{2}$$

where $u_i = u_i(\mathbf{x}, t)$ is the prescribed velocity on the surface A, and the radiation conditions at infinity are

$$v_i(\mathbf{x}, t) = O(1/x) \,,$$
$$p(\mathbf{x}, t) = O(1/x^2) \,, \tag{3}$$

as $x \to \infty$, where $x = \|\mathbf{x}\|_2$ is the Euclidean distance from the origin $O(x_1, x_2, x_3)$. It is known that, while the corresponding unsteady Navier-Stokes equation is Galilei invariant, the time-dependent Stokes Eq. (1) is not (Bührle, 2007). However, the difference between the solutions of Eq. (1) obtained in two Galilei reference frames may be negligible in many practical computations and, then, it does not matter in which of them the time-dependent Stokes equations system is solved, e.g. in the laboratory or in the body coordinate systems, as long as both are nearly truly inertial reference frames. Moreover, the (time-dependent) Stokes equations system

(3) is valid for small oscillation amplitudes of angular frequency ω, such that the body position is always inside the range of the viscous length $L_\nu = (\nu/\omega)^{1/2}$, which is roughly the distance up to which the flow spreads over one oscillation period, where $\nu = \mu/\rho$ is the kinematic fluid viscosity.

2.2 Green function for the time-dependent Stokes equations system

As all variables are assumed as sinusoidal functions of the (imposed) oscillation frequency ω, when an oscillating point force $\mathbf{b} = \delta(\mathbf{x} - \mathbf{y})e^{I\omega t}$ is located at the source point $\mathbf{y} = (y_1, y_2, y_3)$, then, the velocity and pressure are assumed to be $\mathbf{v}(\mathbf{x})e^{I\omega t}$ and $p(\mathbf{x})e^{I\omega t}$, respectively, where, $\mathbf{x} = (x_1, x_2, x_3)$ is the field point, $\mathbf{b} = (b_1, b_2, b_3)$ is the unit body force along the unit direction $\mathbf{b}^0$, while $\delta(\mathbf{x} - \mathbf{y})$ is the Dirac function, and I is the imaginary unit. Then, the time-dependent Stokes equations system (3) is rewritten in the frequency domain as (e.g. Wang, 2002, Sec. 4.3, p. 57)

$$
\begin{aligned}
\rho(I\omega)v_j &= -\nabla_j p + \mu\nabla^2 v_j + b_j\delta(\mathbf{x} - \mathbf{y}) \,, \\
\nabla_j v_j &= 0 \,.
\end{aligned}
\tag{4}
$$

Solving Eq. (4) leads

$$
\begin{aligned}
v_i(\mathbf{x}, \mathbf{y}) &= \alpha g_{ij}(\mathbf{x}, \mathbf{y})b_j && \text{velocity;} \\
p(\mathbf{x}, \mathbf{y}) &= \alpha q_j(\mathbf{x}, \mathbf{y})b_j && \text{pressure;} \\
t_i(\mathbf{x}, \mathbf{y}) &= T_{ijk}(\mathbf{x}, \mathbf{y})n_k b_j && \text{traction;}
\end{aligned}
\tag{5}
$$

with $\alpha = -1/(8\pi)$ and T_{ijk} the stress tensor. The Green functions are given by (e.g. Pozrikidis, 1996, Sec. 6.14, p. 301)

$$
\begin{aligned}
g_{ij}(\mathbf{x}, \mathbf{y}) &= A(\xi)\frac{\delta_{ij}}{r} + C(\xi)\frac{r_i r_j}{r^3} \,, \\
q_j(\mathbf{x}, \mathbf{y}) &= 2\frac{r_j}{r^3} \,,
\end{aligned}
\tag{6}
$$

where δ_{ij} is the Kronecker delta, which is 1 if $i = j$ and 0 otherwise, and the (complex) coefficients are

$$
\begin{aligned}
A(\xi) &= 2e^{-\xi}\left(1 + \frac{1}{\xi} + \frac{1}{\xi^2}\right) - \frac{2}{\xi^2} \,, \\
C(\xi) &= -2e^{-\xi}\left(1 + \frac{3}{\xi} + \frac{3}{\xi^2}\right) - \frac{6}{\xi^2} \,,
\end{aligned}
\tag{7}
$$

and

$$
\begin{aligned}
\xi &= \chi r \,, \\
\chi &= (-I\omega/\nu)^{1/2} \,, \\
r &= \|\mathbf{r}\|_2 \,, \\
\mathbf{r} &= \mathbf{x} - \mathbf{y} \,, \\
I &: \text{imaginary unit.}
\end{aligned}
\tag{8}
$$

The Green functions given by Eq. (6) are very similar to those of the steady flow, although with frequency dependent kernels. As it is known, $A(0) = C(0) = 1$, which suggests that at small frequencies or close to the point force, the Green functions for the oscillating creeping flow reduces to the ones of the steady creeping flow (Kim and Karrila, 1991; Pozrikidis, 1997). The stress tensor T_{ijk} associated with Eq. (5) is found using (e.g. Ladyzhenskaya, 1969, Sec. 3.2, p.
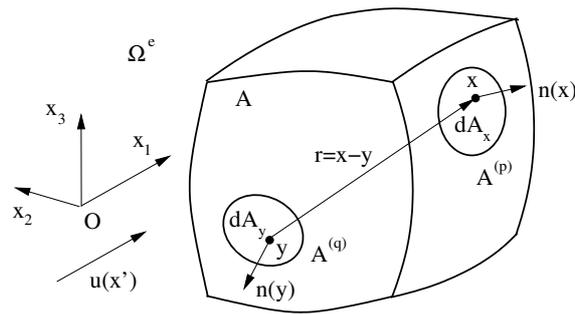
Figure 1: Sketch of a closed and piecewise smooth surface A with an exterior flow domain Ω^e: the field point $\mathbf{x}$, the source point $\mathbf{y}$, the relative position $\mathbf{r} = \mathbf{x} - \mathbf{y}$, the unit normals $\mathbf{n}(\mathbf{x}), \mathbf{n}(\mathbf{y})$, and the differential areas $dA_{\mathbf{x}}, dA_{\mathbf{y}}$.

53)

$$T_{ijk}(q_j, g_{ij}) = \delta_{ik}q_j + \mu \left(\frac{\partial g_{ij}}{\partial x_k} + \frac{\partial g_{kj}}{\partial x_i} \right) . \tag{9}$$

Introducing Eq. (6) into Eq. (9) and replacing in Eq. (5), after some algebra results,

$$t_{ij} = -\frac{\alpha}{r^2} \left(a_{ij} + b_{ij} + c_{ij} \right) , \tag{10}$$

being

$$\begin{aligned}
a_{ij} &= c_1 h \delta_{ij} , \\
b_{ij} &= c_1 r_i^0 n_j^0 + c_2 n_i^0 r_j^0 , \\
c_{ij} &= c_3 h r_i^0 r_j^0 ,
\end{aligned} \tag{11}$$

where $\mathbf{r}^0 = \mathbf{r}/\|\mathbf{r}\|_2$ is the unit vector along the relative distance $\mathbf{r}$, n_k^0 is the unit normal at the source point $\mathbf{y}$, while $h = r_k^0 n_k^0$, and

$$\begin{aligned}
c_1 &= C - A + \tilde{A} , \\
c_2 &= 2(C - 1) , \\
c_3 &= 2\tilde{C} - 6C ,
\end{aligned} \tag{12}$$

with $\tilde{A}$ and $\tilde{C}$ given in Eq. (7), while

$$\begin{aligned}
\tilde{A}(\xi) &= -2e^{-\xi} \left(1 + \xi + \frac{2}{\xi} + \frac{2}{\xi^2} \right) + \frac{4}{\xi^2} , \\
\tilde{C}(\xi) &= 2e^{-\xi} \left(3 + \xi + \frac{6}{\xi} + \frac{6}{\xi^2} \right) - \frac{12}{\xi^2} .
\end{aligned} \tag{13}$$

Equations (10-13) look a little different from the standard ones found in literature (Pozrikidis, 1997). Nevertheless, it was verified that they are equivalent through a numerical computation.

3 NUMERICAL FORMULATION

3.1 Indirect boundary integral equation of Fredholm type and second kind

A modified version of the so-called "completed double-layer boundary integral equation method", e.g. see Power and Wrobel (1995), Sec. 6.2, p. 196, or Kim and Karrila (1991), was proposed in a previous work (D'Elía et al., 2009b). In the remaing paragraphs of this section the modified version is summarized.

The velocity field $v_i(\mathbf{x})$ is thought as a linear superposition of the velocity field produced by a double-layer potential $w_i^{\mathrm{DL}}(\mathbf{x}; \boldsymbol{\psi})$ plus a single-layer (SL) one $w_i^{\mathrm{SL}}(\mathbf{x}; \boldsymbol{\phi})$, i.e.

$$v_i(\mathbf{x}) \equiv v_i(\mathbf{x}; \boldsymbol{\psi}; \boldsymbol{\phi}) = w_i^{\mathrm{DL}}(\mathbf{x}; \boldsymbol{\psi}) + w_i^{\mathrm{SL}}(\mathbf{x}; \boldsymbol{\phi}) \qquad \text{for all } \mathbf{x} \in \Omega^e. \tag{14}$$

The perturbation velocity from the exterior side of the surface A, see Fig. 1, is given by

$$v_i(\mathbf{x}) = w_i^{\mathrm{DL}}(\mathbf{x}; \boldsymbol{\psi})_{(e)} + w_i^{\mathrm{SL}}(\mathbf{x}; \boldsymbol{\psi})_{(e)} \qquad \text{for all } \mathbf{x} \in A. \tag{15}$$

On one hand, the velocity potential due to a double-layer surface density $\psi(\mathbf{y})$ is defined as

$$w_i^{\mathrm{DL}}(\mathbf{x}; \boldsymbol{\psi}) = \int_A \mathrm{d}A_{\mathbf{y}} \; K_{ij}(\mathbf{x}, \mathbf{y}) \psi_j(\mathbf{y}) \,,$$
$$\text{with} \quad K_{ij}(\mathbf{x}, \mathbf{y}) = -\frac{3}{4\pi} \frac{r_i r_j r_k}{r^5} n_k(\mathbf{y}) \,. \tag{16}$$

If the density $\psi_j(\mathbf{y})$ is smooth enough, it is known that the double-layer velocity $w_i^{\mathrm{DL}}(\mathbf{x}; \boldsymbol{\psi})$ verifies the jump property (e.g. Ladyzhenskaya, 1969, Sec. 3.2, Eq. 22, p. 57),

$$\mathbf{w}^{\mathrm{DL}}(\mathbf{x}; \boldsymbol{\psi})_{(i)} - \mathbf{w}^{\mathrm{DL}}(\mathbf{x}; \boldsymbol{\psi})_{(e)} = \boldsymbol{\psi}(\mathbf{x}) \,, \tag{17}$$

across the single closed surface A when $\mathbf{x} \in A$, where subscripts (i) and (e) denote the limiting values of $\mathbf{w}^{\mathrm{DL}}(\mathbf{x}; \boldsymbol{\psi})$ on the surface A, in case this surface is approached from inside or outside, respectively, and given by

$$w_i^{\mathrm{DL}}(\mathbf{x}; \boldsymbol{\psi})_{(i)} = +\frac{1}{2}\psi_i(\mathbf{x}) + w_i^{\mathrm{DL}}(\mathbf{x}; \boldsymbol{\psi}) \,,$$
$$w_i^{\mathrm{DL}}(\mathbf{x}; \boldsymbol{\psi})_{(e)} = -\frac{1}{2}\psi_i(\mathbf{x}) + w_i^{\mathrm{DL}}(\mathbf{x}; \boldsymbol{\psi}) \,, \tag{18}$$

where $w_i^{\mathrm{DL}}(\mathbf{x}; \boldsymbol{\psi})$ denotes the direct value of $w_i^{\mathrm{DL}}(\mathbf{x}; \boldsymbol{\psi})$ on the surface A.

On the other hand, the velocity potential of a single-layer surface density $\phi(\mathbf{y})$ is defined as

$$w_i^{\mathrm{SL}}(\mathbf{x}; \boldsymbol{\phi}) = \int_A \mathrm{d}A_{\mathbf{y}} \; \tilde{S}_{ij}(\mathbf{x}, \mathbf{y}) \phi_j(\mathbf{y}) \,,$$
$$\text{where} \quad \tilde{S}_{ij}(\mathbf{x}, \mathbf{y}) = -\frac{1}{8\pi\mu} \left[\frac{\delta_{ij}}{r} + \frac{r_i r_j}{r^3} \right] \,. \tag{19}$$

In order to exclude the rigid body motions, the (arbitrary) linear dependence

$$\phi_i(\mathbf{y}) = c \, \delta_{ij} \psi_j(\mathbf{y}) \qquad \text{with } c = \rho_1 U_1, \tag{20}$$

is chosen (Hebeker, 1986; Pozrikidis, 1997), where ρ_1 and U_1 and are the unit fluid density and unit speed, respectively. The conversion factor c is introduced since both layer densities ϕ and ψ have different physical dimensions, that is, ϕ constitutes a force surface density (or pressure), e.g. $\mathrm{N/m}^2$, while ψ is a perturbation velocity, e.g. ms^{-1}. Then,

$$\phi_j(\mathbf{y}) = c \, \psi_j(\mathbf{y}) \,, \tag{21}$$

and the perturbation velocity due to a single-layer potential is rewritten as

$$w_i^{\mathrm{SL}}(\mathbf{x}; \boldsymbol{\psi}) = \int_A \mathrm{d}A_{\mathbf{y}} \; S_{ij}(\mathbf{x}, \mathbf{y}) \psi_j(\mathbf{y}) \,, \tag{22}$$

where now

$$S_{ij}(\mathbf{x}, \mathbf{y}) = -\frac{U_1}{8\pi\nu_1}\left[\frac{\delta_{ij}}{r} + \frac{r_i r_j}{r^3}\right] , \tag{23}$$

is the "kinematic" Stokeslet kernel, and $\nu_1 = \mu_1/\rho_1$ is the unit kinematic fluid viscosity. The perturbation velocity from the exterior side of the surface A is given by Eq. (14) and, taking into account the first boundary condition in Eq. (2),

$$w_i^{\mathrm{DL}}(\mathbf{x}; \boldsymbol{\psi})_{(e)} + w_i^{\mathrm{SL}}(\mathbf{x}; \boldsymbol{\psi})_{(e)} = -u_i(\mathbf{x}) \qquad \text{for all } \mathbf{x} \in A. \tag{24}$$

Using the exterior limit case of Eq. (18) and replacing by Eq. (23), Eq. (24) gives

$$-\frac{1}{2}\psi_i(\mathbf{x}) - \int_A \mathrm{d}A_\mathbf{y} \; [K_{ij}(\mathbf{x}, \mathbf{y}) - S_{ij}(\mathbf{x}, \mathbf{y})]\,\psi_j(\mathbf{y}) = -u_i(\mathbf{x}) \qquad \text{for all } \mathbf{x} \in A. \tag{25}$$

After some algebra, the modified version is written as the boundary integral equation

$$\int_A \mathrm{d}A_\mathbf{y} \; \{[S_{ij}(\mathbf{x}, \mathbf{y}) - K_{ij}(\mathbf{x}, \mathbf{y})]\,\psi_j(\mathbf{y}) + K_{ij}(\mathbf{x}, \mathbf{y})\psi_j(\mathbf{x})\} = -u_i(\mathbf{x}) \quad \text{for all } \mathbf{x} \in A, \tag{26}$$

for the double-layer surface density $\boldsymbol{\psi}$, with $i, j = 1, 2, 3$, where $\mathrm{d}A_\mathbf{y} = \mathrm{d}A(\mathbf{y})$ is the differential area. As it is known in the Green function theory, as well as in solid and fluid mechanics, the j column of the tensor $K_{ij}(\mathbf{x}, \mathbf{y})$ physically represents the perturbation velocity induced by a double surface layer density of unit value on the j-component only. Using matrix notation, Eq. (26) is rewritten as

$$\mathbf{g}(\mathbf{x}) + \mathbf{u}(\mathbf{x}) = \mathbf{0} \qquad \text{for all } \mathbf{x} \in A, \tag{27}$$

which is a boundary integral equation of Fredholm type and second kind, with source term $-\mathbf{u}(\mathbf{x})$, where $\mathbf{u}(\mathbf{x})$ is the unperturbed flow velocity field, whereas

$$\mathbf{g}(\mathbf{x}) \equiv \int_A \mathrm{d}A_\mathbf{y} \; [\mathbf{H}(\mathbf{x}, \mathbf{y})\boldsymbol{\psi}(\mathbf{y}) + \mathbf{K}(\mathbf{x}, \mathbf{y})\boldsymbol{\psi}(\mathbf{x})] \qquad \text{for all } \mathbf{x} \in A, \tag{28}$$

is a boundary integral operator with kernels $\mathbf{H}(\mathbf{x}, \mathbf{y})$ and $\mathbf{K}(\mathbf{x}, \mathbf{y})$, with $\mathbf{H}(\mathbf{x}, \mathbf{y}) = \mathbf{S}(\mathbf{x}, \mathbf{y}) - \mathbf{K}(\mathbf{x}, \mathbf{y})$. These kernels couple the double-layer surface density $\boldsymbol{\psi}$ at the integration point $\mathbf{y}$ and at the field point $\mathbf{x}$.

Equation (26) was already used in steady flows in (D'Elía et al., 2009b), and solved using both a collocation technique and a GBEM. In the last case, details about a systematic strategy for a numerical quadrature computing the related double surface integrals can be found in Taylor (2003); D'Elía et al. (2009a).

z	1	2	3	4	5	6	7	8	9
N	26	98	218	386	602	866	1178	1538	2402
E	48	192	432	768	1200	1728	2352	3072	4800

Table 1: Number of nodes N and elements E. Meshes 2-9 are structured on the unit sphere and on the unit cube.
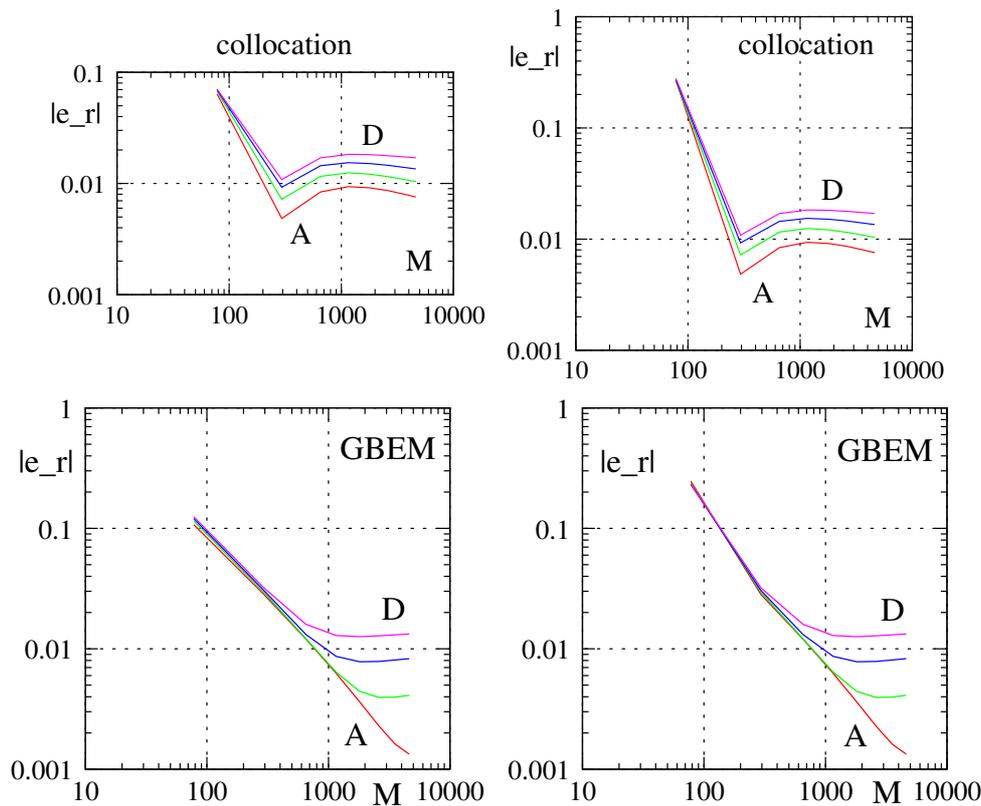
Figure 2: Absolute value of the relative error $|e_r|$ of the force coefficient K_i as function of the number of degrees of freedom M and the frequency ω on the unit sphere with the Q_{22} quadrature rule at frequencies $\omega = [\ 0.4,\ 0.7,\ 1.0,\ 1.3\ ]$ rad/s (curves $A - D$): uniform flow K_1 (left) and shear flow $\tilde{K}_3$ (right). Collocation (top) and GBEM (bottom).

4 NUMERICAL EXAMPLES

Two unsteady flow cases are considered: a sphere of unit radius and a cube of unit edge length, at rest in their body inertial frames and whose centers are placed at the origin of the Cartesian coordinate system in $\mathbb{R}^3$. Both bodies are immersed in a viscous and incompressible fluid of Newtonian type that extends indefinitely. In the numerical simulations, the following values are adopted: fluid density $\rho = 1$ kg/m^3 and kinematic viscosity $\nu = 1$ m^2/s.

The number z of BEM meshes and the corresponding number of nodes N and number of elements E are shown in Table 1, where meshes 2-9 are structured (smooth). The Gauss-Legendre formula is employed in the modified Taylor "black box" integrator, with n_{1d} quadrature points along each direction which, in turn, implies a total of n_{1d}^4 points by interaction pair. A Q_{22} rule is used for the number of quadrature points among the panel layers, meaning that there are 2 Gauss-Legendre points on the self-integral and the first layer of neighbouring panels and 2 points for the remaining layers.

The drag coefficients are obtained from the force $\mathbf{D} = (D_1, D_2, D_3)$ and torque $\mathbf{T} = (T_1, T_2, T_3)$ as $K_i = D_i/(\mu U_\infty L)$ and $\tilde{K}_i = C_i/(\mu U_\infty L^2)$, where U_∞ is the (unperturbed) incoming speed, and L is a typical length. The subindex $i = 1, 2, 3$ in the drag coefficients indicates the corresponding x_i Cartesian component. The absolute value of the relative error $|e_r|$ for the force coefficient K_i is computed as $|e_r| = |K_{i,\text{num}}/K_{i,\text{(semi)analytical}} - 1|$, and it is plotted as a function of the number M of the degrees of freedom, being $M = 3E$ and $M = 3N$ in collocation and Galerkin, respectively.
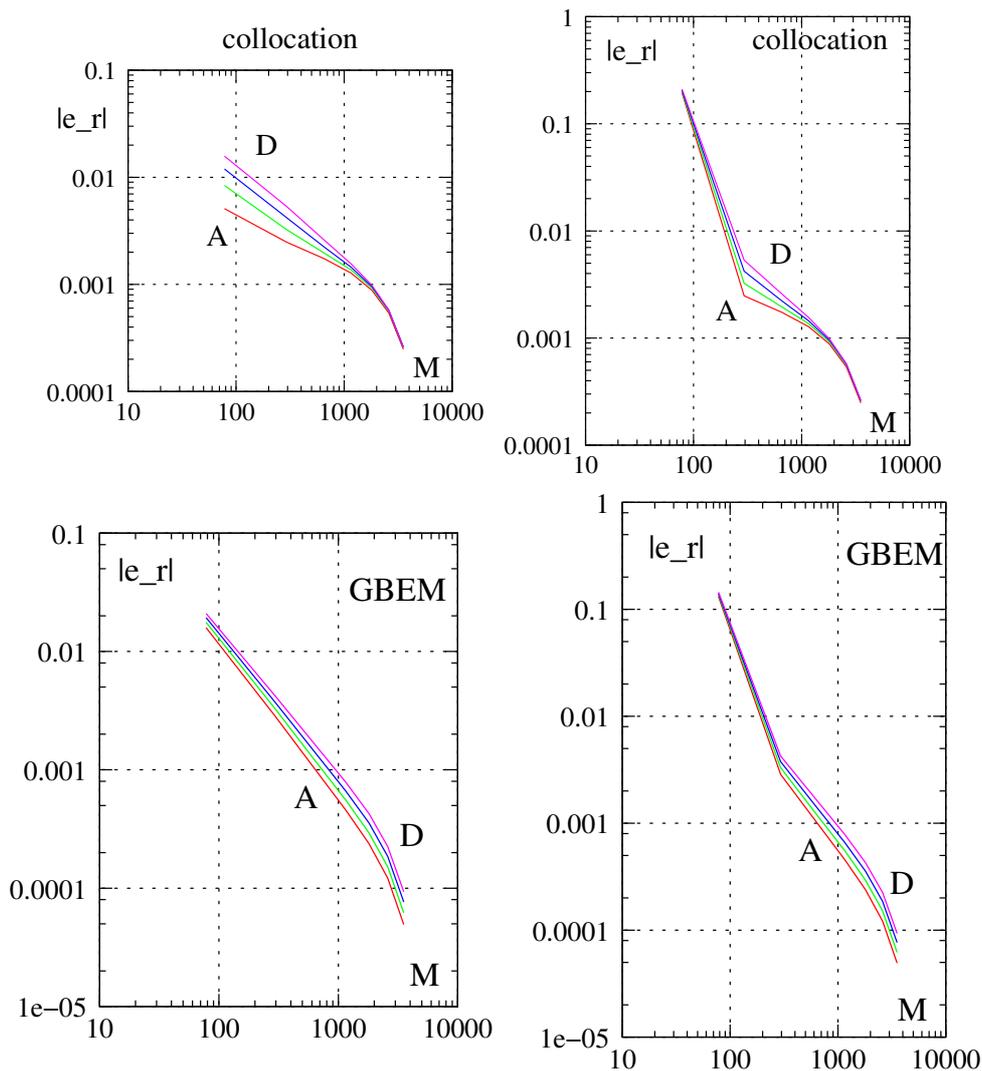
Figure 3: Absolute value of the relative error $|e_r|$ of the force coefficient K_i as function of the number of degrees of freedom M and the frequency ω on the unit cube with the Q_{22} quadrature rule at frequencies $\omega = [\,0.4,\ 0.7,\ 1.0,\ 1.3\,]$ rad/s (curves $A - D$): uniform flow K_1 (left) and shear flow $\tilde{K}_3$ (right). Collocation (top) and GBEM (bottom).

The numerical examples cover issues on the convergence of the numerical solution under mesh refinement and, in the first test case, a comparison against the analytical values as a function of the imposed vibrating frequency. Flat simplex triangles are used in all cases.

4.1 Sphere

Tests with spheres are extensively used in experimental oscillating flows (Klotsa, 2009). The sphere test case is chosen since there are analytical solutions for some flow conditions. For instance, the following analytical relations are known (Padmavathi, 2010; Venkatalaxmi et al., 2004; Kim and Karrila, 1989; Pozrikidis, 1989):

1. When the sphere performs translational oscillations with perturbation velocity $\hat{\mathbf{U}}e^{I\omega t}$ in the fluid at rest, the drag is given by

$$\mathbf{D} = 6\pi\mu a \left(1 + \lambda + \lambda^2/9\right) \hat{\mathbf{U}}\,. \tag{29}$$

2. When the sphere performs a rotational oscillation with spin perturbation $\hat{\mathbf{\Omega}}e^{I\omega t}$ in the fluid at rest, the torque is given by

$$\mathbf{T} = 8\pi\mu a^3 \frac{1 + \lambda + \lambda^2/3}{1 + \lambda}\hat{\mathbf{\Omega}} \,. \tag{30}$$

3. When the fluid perform an oscillation with velocity $\hat{\mathbf{U}}_\infty(\mathbf{x})e^{I\omega t}$ around the sphere at rest, where $\hat{\mathbf{U}}_\infty(\mathbf{x})$ is an unperturbed velocity field such that $[\nabla^2\hat{\mathbf{U}}_\infty(\mathbf{x})]_0 = \mathbf{0}$, the drag and torque are given by

$$\begin{aligned}
\mathbf{D} &= 6\pi\mu a \left(1 + \lambda + \lambda^2/3\right)\left[\hat{\mathbf{U}}_\infty(\mathbf{x})\right]_0 \,, \\
\mathbf{T} &= 4\pi\mu a^3 \frac{e^\lambda}{1 + \lambda}\left[\nabla \times \hat{\mathbf{U}}_\infty(\mathbf{x})\right]_0 \,.
\end{aligned} \tag{31}$$

In Eqs. (29-31), the non-dimensional coefficient is $\lambda = \chi a$, and χ is defined in Eq. (8), while $[...]_0$ is the evaluation at the centre of the sphere. The sphere radius is $a = 1$ m and the unperturbed flow conditions are: uniform $\hat{\mathbf{U}}_\infty(\mathbf{x}) = (U_\infty, 0, 0)$, and shear $\hat{\mathbf{U}}_\infty(\mathbf{x}) = U_\infty(x_2, -x_1, 0)/a$. In Fig. 2 the absolute value of the relative error $|e_r|$ of the force coefficient K_i on the unit sphere, using the Q_{22} quadrature rule is plotted for the translational oscillation at frequencies at frequencies $\omega = [\,0.4,\ 0.7,\ 1.0,\ 1.3]$ rad/s (curves $A - D$) for uniform flow K_1 (left) and shear flow $\tilde{K}_3$ (right), collocation (top) and GBEM (bottom).

4.2 Cube

As an example of a sharp body, a cube of unit edge length $L = 1$ m, whose center is placed at the origin in $\mathbb{R}^3$, is considered. The cube test case is selected as a crude simplification of the phenomena appearing with MEMS geometries (Fachinotti et al., 2007; Méndez et al., 2008; Berli and Cardona, 2009). Since there is no analytical solution for the unit cube, the relative errors are computed taking as reference the results from the more refined mesh, in this case mesh 9, see Table 1. In Fig. 3 the absolute value of the relative error $|e_r|$ of the force coefficient K_i on the unit cube, using the Q_{22} quadrature rule is plotted for the translational oscillation at frequencies $\omega = [\,0.4,\ 0.7,\ 1.0,\ 1.3]$ rad/s (curves $A - D$) for uniform flow K_1 (left) and shear flow $\tilde{K}_3$ (right), collocation (top) and GBEM (bottom).

5 CONCLUSIONS

An indirect boundary integral equation of Fredholm type and second kind has been employed for unsteady creeping flow exterior to a three-dimensional rigid body at rest in an incompressible and viscous fluid of Newtonian type, and it was numerically solved using collocation and Galerkin procedures. The boundary integral equation has been chosen as a combination of double- and single- layer potentials for time-harmonic creeping flows with densities defined over the closed surface. It is an extension of a previous work (D'Elía et al., 2009b), where a modification of the so-called "completed double-layer boundary integral equation method" (Power and Wrobel, 1995; Kim and Karrila, 1991) was proposed. It was checked that when the frequency tends to zero, the drag coefficient of the oscillating creeping flow reduces to the steady one. A Q_{22} rule was employed in the numerical examples, with $n_{1d} = 2$ Gauss-Legendre points on the self-integral and first layer of neighbouring panels, those that have a common edge or vertex, and $n_{1d} = 2$ for the remaining layers on each integration coordinate, which,

in turn, imply a total of n_{1d}^4 points by pair interaction. The numerical examples included the translational and rotational oscillations of the fluid with an harmonic time dependence around the sphere of unit radius and around the cube of unit edge length, both at rest, at frequencies $\omega = [\, 0.4, \; 0.7, \; 1.0, \; 1.3\,]$ rad/s (curves $A - D$ in Figs. 2-3), for the force coefficients K_1 (uniform flow) and $\tilde{K}_3$ (shear flow). In the sphere case, it was noted that at the present time there is divergence under mesh refinement for frequencies ω greater to the unity, and it worst with a collocation technique than with a Galerkin one. In the cube case, the convergence under mesh refinement was verified although the relative errors were computed taking as reference the results from the more refined mesh (mesh 9), since there is no analytical solution. The failure at high frequencies is mainly due to the following. It is known that the first term in an asymptotic series for high frequencies of the transient Stokeslet is the steady potential dipole (Pozrikidis, 1997). This fact suggests that a transient Stokeslet at high frequencies produces an irrotational flow field. Then, in order to fix the divergence in the solution for higher frequencies, the present BEM should be extended to model the velocity field of the steady potential dipole (inviscid flow), whose order of singularity is two units greater than the steady Stokeslet. Future work could be focused in this issue.

REFERENCES

Berli C. and Cardona A. On the calculation of viscous damping of microbeam resonators in air. *Journal of Sound and Vibration*, 327(1-2):249–253, 2009.

Bonnet M., Maier G., and Polizzotto C. Symmetric Galerkin boundary element methods. *Appl. Mech. Rev.*, 51(11):669–704, 1998.

Bührle J. *Properties of time-dependent Stokes flow and the regularization of velocity fluctuations in particle suspensions*. Ph.D. thesis, Fachbereich Physik der Philipps, Universität Marburg, Germany, 2007.

D'Elía J., Battaglia L., Cardona A., and Storti M. Full numerical quadrature of weakly singular double surface integrals in Galerkin boundary element methods. *Comm. Numer. Meth. Engng.*, 2009a. Doi:10.1002/cnm.1309, in press.

D'Elía J., Battaglia L., Storti M., and Cardona A. Galerkin boundary integral equations applied to three dimensional Stokes flows. In Bauza, Lotito, Parente, and Vénere, editors, *Mecánica Computacional, vol. XXVIII*, pages 1453–1462. Tandil, 2009b.

Fachinotti V., Cardona A., D'Elía J., and Paquay S. BEM for the analysis of fluid flow around MEMS. In S.A. Elaskar, E.A. Pilotta, and G.A. Torres, editors, *Mecánica Computacional, vol. XXIV*, pages 1104–1119. Córdoba, Argentina, 2007.

Hebeker F.K. Efficient boundary element methods for three-dimensional exterior viscous flow. *Num. Meth. PDE*, pages 273–297, 1986.

Kim S. and Karrila S.J. Integral equations of second kind for Stokes flow: direct solutions for physical variables and removal of inherent accuracy limitations. *Chem. Eng. Comm.*, 82:123–161, 1989.

Kim S. and Karrila S.J. *Microhydrodynamics: Principles and Selected Applications*. Butterwoth-Heinemann, 1991.

Klotsa K.D. *The dynamics of spheres in oscillatory fluid flows*. Ph.D. thesis, University of Nottingham, England, 2009.

Ladyzhenskaya O.A. *The Mathematical Theory of Viscous Incompressible Flow*. Gordon and Breach Science Publishers, 2 edition, 1969.

Méndez C., Paquay S., Klapka I., and Raskin J.P. Effect of geometrical nonlinearity on MEMS thermoelastic damping. *Nonlinear Analysis: Real World Applications*, 10(3):1579–1588, 2008.

Padmavathi B.S. personal communication, 2010.

Power H. and Wrobel L. *Boundary Integral Methods in Fluid Mechanics*. Computational Mechanics Publications, Southampton,UK, 1995.

Pozrikidis C. A singularity method for unsteady linearized flow. *Physics of Fluids A*, 1(9):1508–1520, 1989.

Pozrikidis C. *Introduction to Theoretical and Computational Fluid Dynamics*. Oxford, 1996.

Pozrikidis C. *Boundary Integral and Singularity Methods for Linearized Viscous Flow*. Cambridge University Press, 1997.

Sutradhar A., Paulino G.H., and Gray L.J. *Symmetric Galerkin Boundary Element Method*. Springer, 2008.

Taylor D.J. Accurate and efficient numerical integration of weakly singulars integrals in Galerkin EFIE solutions. *IEEE Trans. on Antennas and Propag.*, 51(7):1630–1637, 2003.

Venkatalaxmi A., Padmavathi B.S., and Amaranath T. A general solution of unsteady Stokes equations. *Fluid Dynamics Research*, 35:229–236, 2004.

Wang X. *Fast Stokes: A Fast 3-D Fluid Simulation Program for Micro-Electro-Mechanical Systems*. Ph.D. thesis, MIT, 2002.